Journal of Quantitative Spectroscopy & Radiative Transfer 112 (2011) 1961–1966

Contents lists available at ScienceDirect

Journal of Quantitative Spectroscopy & Radiative Transfer

journal homepage: www.elsevier.com/locate/jqsrt

Acetonitrile (CH_3CN) infrared absorption cross sections in the 3 μm region

Nicholas D.C. Allen *, Jeremy J. Harrison, Peter F. Bernath

Department of Chemistry, University of York, Heslington, York YO10 5DD, United Kingdom

ARTICLE INFO

Article history:
Received 15 February 2011
Received in revised form
4 April 2011
Accepted 7 April 2011
Available online 14 April 2011

Keywords:
Acetonitrile
Atmospheric science
High resolution Fourier transform spectroscopy
Infrared absorption cross sections
Remote sensing

ABSTRACT

High resolution infrared absorption cross sections of acetonitrile have been determined from spectra recorded in the 3 μm spectral region using a Bruker IFS 125 HR Fourier transform spectrometer (FTS) and a multipass White cell. The eleven synthetic air-broadened acetonitrile spectra were recorded at a resolution of 0.015 cm^{-1} (calculated as 0.9/MOPD (Maximum Optical Path Difference), the Bruker definition of resolution) over a range of different temperatures and pressures that are representative of conditions in the Earth's atmosphere (50–760 Torr and 207–296 K). Intensities were calibrated using infrared spectra recorded at the Pacific Northwest National Laboratory (PNNL). These new cross sections will enable satellite retrievals of acetonitrile in the 3 μm region from atmospheric spectra recorded by satellite instruments, such as the ACE (Atmospheric Chemistry Experiment)-FTS.

1. Introduction

Acetonitrile (CH_3CN), which has multiple synonyms that include methyl cyanide, cyanomethane and ethanenitrile, is a trace gas with a highly variable atmospheric concentration [1,2]. Acetonitrile is known to be toxic and emissions from industrial processes and vehicles are carefully regulated. The predominant source of acetonitrile is through biomass burning emissions, which are thought to contribute up to 90% of the total atmospheric loading [3,4]. Thus acetonitrile is potentially an important tracer gas for identifying biomass burning plumes.

It has been estimated that 4.7 Pg of carbon are emitted from biomass burning sources within the equatorial region each year leading to the creation of a host of volatile organic compounds [3]. With 80% of biomass burning occurring in the tropics [4] significant loss of nitrogen nutrients could have a large impact on tropical ecosystems and environments [5].

The budget of acetonitrile is poorly understood and not well constrained [6]. Early measurements had wildly differing volume mixing ratios (VMRs) with background concentrations up to 7 parts per billion (ppb) [7,8]. This is partially due to high variability at low altitudes, a result of local influences. There is also a lack of knowledge about the main sink mechanisms making the lifetime difficult to estimate. The reaction with hydroxyl radicals is slow; the lifetime of acetonitrile is suggested to be in the order of 6–12 months [6,9]. In the stratosphere acetonitrile reacts with hydroxyl radicals [1,10], acting as a sink and a potential precursor to hydrogen cyanide [11], and is also believed to react with atomic oxygen in the mesosphere [12,13]. Below the tropopause mixing ratios of acetonitrile are significantly higher, between 150 and 200 ppt [8]. Uptake of acetonitrile by the ocean has been suggested as an important sink in the troposphere, particularly in regions of strong upwelling [14] and low sea temperature, such as the southwest coast of Africa [1,15].

There is good evidence of an ocean sink including an observed decline in acetonitrile concentrations in the marine boundary layer relative to other trace gases that do not have an ocean sink [15,16]. Nevertheless there is still a significant debate as to the exact sink pathway; dry

* Corresponding author. Tel.: +44 1904 434525; fax: +44 1904 432516.
E-mail address: ndca500@york.ac.uk (N.D.C. Allen).

0022-4073/$ - see front matter © 2011 Elsevier Ltd. All rights reserved.
doi:10.1016/j.jqsrt.2011.04.001

and wet deposition, as well as a bacterial degradation process have been suggested [9,17]. Bange and Williams [17] have suggested prehistoric atmospheres lacking oxygen may have had bacterial enzymes that converted nitriles into ammonia as a source of energy. Such enzymes have been isolated in ocean beds and may still be globally abundant.

Acetonitrile concentrations are greatest near the equator, where biomass burning activity is most prevalent. A biomass burning source of approximately 0.5–1.5 Tg yr^{-1} [3,4,9] out of an estimated 1.6 Tg yr^{-1} total tropospheric acetonitrile source [8] supports this theory. A strong correlation between acetonitrile and carbon monoxide is observed [3] as both species are produced in the cooler smouldering phase of biomass burning [2], although the relationship is also dependent upon the fuel type [14]. The linear correlation breaks down in clean background boundary layer air, where acetonitrile concentrations decline [9].

A sizeable inter-hemispheric asymmetry is observed, possibly as a result of continental outflow [6]. Heightened acetonitrile concentrations have been detected in plumes emitted from continental Africa and Asia in conjunction with other biomass tracers [2,9]. The highest acetonitrile mixing ratios are encountered in the tropical lower stratosphere, where acetonitrile permeates the tropical tropopause and enters from the free troposphere [12]. However, strong advection and convection effects, caused by events such as thunderstorms, can lead to the uplift and injection of pollution and acetonitrile enhanced air masses into the stratosphere [18].

The first atmospheric studies of acetonitrile were indirect and concentrations were inferred from stratospheric positive ion clusters, in which acetonitrile is a ligand and displaces water [10,19–21]. Early studies found acetonitrile to be a constituent of vehicle exhaust emissions [1,7,8] and it was used as a fumigant [9], as well as a solvent in industrial polymerisation processes [1,14]. However, changes in practices and new regulations have led more recent studies to suggest that anthropogenic emissions are insignificant relative to biomass burning.

Where background concentrations of acetonitrile are measured, a diurnal cycle in the boundary layer is observed [22] and a strong seasonal variation. Whilst strong enhancements of acetonitrile have been observed in the stratosphere from forest fires [14,18], no significant biogenic sources have been detected [6], and there are no acetonitrile 'point sources' such as industrial sites or power plants [14].

Livesey et al. [12] reported the first retrieval of acetonitrile from space using thermal microwave limb emission of the rotational lines. The first infrared remote sensing measurements of acetonitrile were taken by the MkIV balloon Fourier transform spectrometer (FTS) using the solar occultation technique [11]. These balloon measurements were taken over a number of years between 1993 and 2004 at several locations covering the altitudes from 12 to 30 km. VMRs above the tropopause were found to be between 100 and 150 ppt declining to 40 ppt at 22 km.

Acetonitrile is a molecule of some interest to astronomers and its presence has been detected in a number of objects including molecular clouds and planetary atmospheres [23,24]. Significant acetonitrile concentrations have been measured in the atmosphere of Titan by radio astronomy and it is also likely detectable by infrared spectroscopy [25,26].

To enable the detection of acetonitrile for both atmospheric and planetary applications, high quality spectroscopic data are required. A number of studies have determined molecular parameters for acetonitrile [26–29]. Rinsland et al. [30] recorded a set of quantitative spectra at the PNNL (Pacific Northwest National Laboratory) at a resolution of 0.112 cm^{-1} and a pressure of one atmosphere nitrogen at 276, 298 and 323 K. Nevertheless there is a lack of high resolution spectra recorded over a range of temperatures and pressures appropriate for use in the Earth's atmosphere. PNNL spectra are not suitable for remote sensing of the atmosphere because they do not cover the appropriate pressure range and the resolution is insufficient. Aside from these PNNL measurements and a set of line parameters for the ν_4 band, derived from high resolution room-temperature spectra [31], there is scant acetonitrile data available in the HITRAN database [32]. New high resolution infrared absorption cross sections are necessary for atmospheric applications [30].

Acetonitrile is a symmetric top with C_{3v} symmetry and has moderately strong C–H stretching modes located in the 3.3 μm region. There are many acetonitrile bands in the 3 μm region including the $\nu_2+\nu_8$ band near 2620 cm^{-1}, the weak $2\nu_3$ band observed between 2700 and 2780 cm^{-1}, the $2\nu_6$ band at 2821 cm^{-1}, the ν_1 band centred at 2954 cm^{-1}, the ν_5 band at 3009 cm^{-1} and the $\nu_2+\nu_4$ band at 3179 cm^{-1} [30]. The cross sections determined in this work, recorded at higher resolution and covering a wider range of temperatures and pressures than previous measurements, can be used to retrieve acetonitrile in the troposphere from atmospheric spectra recorded by a number of instruments, in particular the Atmospheric Chemistry Experiment (ACE)-FTS which covers the 750–4400 cm^{-1} region [33]. Due to this extended spectral coverage, it is possible to carry out retrievals in the strong 3.3 μm region, where hydrocarbons have strong intensity modes (C–H stretch) and where there are relatively few spectral interferers. The strongest acetonitrile infrared absorption bands occur near 7 μm, however, these are in close proximity to strong water absorption features.

2. Experimental

The new acetonitrile spectra were recorded at the Molecular Spectroscopy Facility (MSF), Rutherford Appleton Laboratory (RAL) located near Didcot in Oxfordshire, United Kingdom. Using a Bruker IFS 125 HR high resolution FTS, eleven air-broadened acetonitrile absorption spectra were recorded at a resolution of 0.015 cm^{-1} (using the Bruker definition of resolution 0.9/MOPD, the Maximum Optical Path Difference) at temperatures between 207 and 296 K. The spectrometer was equipped with a calcium fluoride (CaF_2) beam splitter and an

indium antimonide (InSb) detector. Using a mid-infrared globar radiation source, in conjunction with an optical filter, F754, the spectral region was restricted to throughput between 2400 and 3500 cm^{-1} to reduce photon shot noise. The diameter of the aperture was set to 2.5 mm. Each recorded interferogram was weakly apodised (Norton–Beer weak) and phase corrected (Mertz). Whilst measurements were recorded the spectrometer was evacuated (below 0.2 Pa) by a set of turbo pumps, minimising the introduction of impurities from trace gases into the optical path. Transfer optics directed the radiation into the sample cell.

The Short Path Absorption Cell (SPAC) [34], a multipass White cell with a base path of 40 cm, is external to the spectrometer and can be operated at temperatures ranging from 77 to 450 K. The mirrors at each end of the SPAC are held in the stainless steel inner pressure vessel and are externally adjustable, hence the path length can easily be altered. The path length of the cell can be set between 1.7 and 19.3 m. The path length is increased for samples at lower temperatures, where the vapour pressure is less, to increase the acetonitrile absorption.

The inner vessel of the cell can be cooled by a surrounding helium-filled cavity and an outer jacket with continuously flowing liquid nitrogen gas, which is controlled by a solenoid valve located on the entrance pipe. To prevent temperature drift an overall vacuum jacket provides insulation and prevents the introduction of impurities into the optical path. Small temperature-controlled electric heaters and six platinum resistance thermometers (PRTs) attached to the cell allow the temperature to be carefully controlled and monitored. For further details about the FTS set-up see Table 1.

UV spectroscopy grade acetonitrile, with a purity $\geq 99.8\%$, was purchased from Fluka. The acetonitrile was placed in a small Pyrex tube where it was repeatedly freeze-pump-thawed to remove dissolved air and impurities. Cold acetonitrile was then introduced slowly into the SPAC through a gas line and dry synthetic air was added to create a suitable mixture. The synthetic air, Air Zero Plus, was purchased from Air Products and consists principally of O_2 ($20.9\% \pm 0.2\%$) and N_2. The overall purity is extremely high at 99.99990% ($H_2O \leq 0.5$, $CH_4 \leq 0.05$, and $CO + CO_2 \leq 0.1$ ppm).

Table 1
FTS settings and SPAC configuration.

Source	Globar (mid-infrared)
Detector	Indium antimonide (InSb)
Beam splitter	Calcium fluoride (CaF_2)
Resolution	0.015 cm^{-1}
Aperture size	2.5 mm
Optical filter	F754 (Northumbria Optical Coatings Ltd.)
Apodisation	Norton–Beer weak
Phase correction	Mertz
Cell windows	Barium fluoride (BaF_2)
Transfer optics	Potassium bromide (KBr)
Mirror coatings	Gold
Pressure gauges	3 MKS-690 A Baratrons (1, 10 and 1000 Torr)
Thermometers	6 Labfacility IEC 751 Class A PRTs

The sample mixture pressures were monitored at all times using three Baratron capacitance manometers (1, 10 and 1000 Torr gauges) which were calibrated by the manufacturer.

Each measurement consisted of a set of air-broadened acetonitrile scans sandwiched between background scans. Background scans were run while the SPAC was evacuated by turbo pumps. The total number of background scan blocks taken (half taken before and half taken after) was the same as the number of sample scan blocks to ensure a good signal-to-noise ratio in the resulting transmission spectra. This also minimised the effects caused by baseline drift over the course of the measurements.

A summary detailing the number of scans in each measurement, along with the pressure, temperature and SPAC path lengths are included in Table 2. At each temperature pure nitrous oxide (N_2O) scans were recorded to calibrate the wavenumber scale of the acetonitrile measurements. The pressure and temperature, as measured by the Baratrons and PRTs throughout each experiment, were logged by computer every few seconds. An average temperature and pressure was determined for each measurement set and variations in these values with time allowed an assessment of their experimental uncertainties. It was found that the pressure fluctuated by less than 0.5% suggesting a highly stable system. Unfortunately the temperature data recorded for measurements warmer than 207 K were lost, as a result of a network error. Nevertheless, at the beginning of each measurement the temperature was recorded manually and in conjunction with the pressure stability, we calculate that the temperature did not fluctuate by more than a degree. This problem was rectified prior to the recording of the lowest temperature measurements, where the partial pressure of the acetonitrile added was the least certain.

Sample conditions at lower temperatures are subject to greater uncertainties in the absorption cross sections. For example, when the SPAC is cooled down the optics and mirrors within the cell shift position as they contract. Therefore whilst the error in the SPAC optical path length is estimated to be $\pm 0.2\%$ at room temperature, this will

Table 2
Summary of experimental conditions for the acetonitrile measurements.

Acetonitrile pressure (Torr)	Total pressure (Torr)	Temperature (K)	Path length (m)[a]	Number of scans[b]
0.034	50.5 ± 0.1	207.6 ± 0.3	19.31	260
0.034	101.5 ± 0.2	207.6 ± 0.2	19.31	240
0.130	50.0 ± 0.1	217 ± 1.0	17.71	310
0.128	99.4 ± 0.2	217 ± 1.0	17.71	150
0.130	248.5 ± 0.4	217 ± 1.0	17.71	300
1.702	201.0 ± 0.2	250 ± 1.0	3.31	300
1.707	401.1 ± 0.4	249 ± 1.0	3.31	300
1.701	601.9 ± 0.5	249 ± 1.0	3.31	300
1.984	370.8 ± 0.6	273 ± 1.0	3.31	300
1.945	599.9 ± 0.6	273 ± 1.0	3.31	300
3.057	760.3 ± 0.7	296 ± 1.0	3.31	270

[a] The optical path length error is estimated to be $\pm 0.2\%$ at room temperature.
[b] An equal number of background scans were also recorded.

likely increase once the cell is cooled down to low temperature. Likewise, the acetonitrile partial pressure at 207 K is difficult to determine. This is because the partial pressure had to be recorded prior to the addition of synthetic air, which led to a small rise in the temperature, which thus in turn increased the partial pressure of the acetonitrile. Measurements of acetonitrile were attempted at both 195 and 200 K; however the partial pressure was not high enough to obtain suitable absorption spectra at the longest SPAC path length. These uncertainties make it necessary to normalise our acetonitrile measurements against a well calibrated intensity standard. The PNNL acetonitrile spectra recorded by Rinsland et al. [30] have been chosen as a reference as discussed in the following section.

Uncertainties in the sample temperature and total pressure range from 0.1% to 0.5% and 0.1% to 0.2%, respectively. As stated previously, the path length error is at least 0.2%. We estimate the photometric uncertainty to be 2%. The PNNL spectra used for calibration have a stated experimental accuracy of 3.5% (1σ). The new acetonitrile spectrum recorded at 296 K and 760.3 Torr was scaled by a factor of 1.006 over the appropriate wavenumber range to bring it into line with the PNNL spectrum at 298 K and 760 Torr. We are confident that the experimental uncertainties are similar for both data sets, and estimate an overall uncertainty in the new acetonitrile cross sections of 4% (1σ).

3. Results and discussion

The following paragraphs detail the generation of acetonitrile absorption cross sections from the initial single channel sample measurements. Firstly, appropriate averages of the acetonitrile single channel sample scans were taken and divided by appropriate averages of the single channel background scans to obtain transmission spectra. The average background scans comprised of an equal number that were taken before and after the sample scans, and this total was equal to the number of sample scans.

Sinusoidal features in the spectral domain, known as channel fringes, were observed in all single channel scans as a consequence of the reflectance of radiation by cell windows and transfer optics leading to the introduction of weak 'echo' centrebursts in the interferogram. Fortunately as these channelling effects were observed in both the single channel background and sample scans they usually cancelled. However, occasionally the channelling oscillations shifted slightly in frequency during the measurements and did not cancel exactly. This problem was encountered for a few of the acetonitrile measurements. For these interferograms the responsible 'echo' centrebursts were carefully removed prior to Fourier transformation into spectra. Care was taken to check that the removal of these 'echo' centrebursts did not introduce errors into the transformed spectra.

Several of the transmission spectra required small baseline corrections, a slight shift in the y-axis, of no more than 0.5%, so that the transmission corresponded to 100% for regions at which there was no absorption. The transmission spectra were then converted into absorption spectra. The x-axis wavenumber scale was calibrated using the pure N_2O spectra recorded intermittently at each temperature during the experimental run. The frequencies of the selected N_2O lines in these pure spectra were compared with the frequencies in the HITRAN 2008 database [32]. According to the HITRAN 2008 database the N_2O lines used for calibration have a wavenumber accuracy of between 0.001 and 0.0001 cm^{-1}. For each temperature, a small correction factor was determined and then applied to the appropriate acetonitrile spectra.

Due to the inherent difficulties in recording acetonitrile spectra at cold temperatures, because of the lower vapour pressure, the measurements were calibrated against acetonitrile absorption spectra recorded by Rinsland et al. [30]. The PNNL composite spectra were recorded by FTS at 276, 298 and 323 K with a White cell at a pressure of 760 Torr of nitrogen. The integrated intensities of the corresponding 3 μm bands at these three temperatures show no temperature dependence. The assumption that this holds true for all of our measurements is a good one for an isolated band comprising primarily of fundamentals.

The y-axis calibration was performed after converting transmission spectra to the HITRAN cross section units of cm^2 $molecule^{-1}$, achieved using the method, as detailed previously in the work of Harrison et al. [35], by the following equation:

$$\sigma(\upsilon,P_{air},T) = -\xi\frac{10^4 k_B T}{Pl}\ln\tau(\upsilon,P_{air},T) \quad (1)$$

where τ (υ, P_{air}, T) is the transmittance at wavenumber υ (cm^{-1}), T is the temperature (K), P_{air} is the synthetic air pressure (Pa), P is the partial pressure of the acetonitrile absorber gas (Pa), l the path length (m), k_B the Boltzmann constant (1.3806504×10^{-23} J K^{-1}) and ξ is the normalising factor which is determined by the equation,

$$\int_{2700\,cm^{-1}}^{3260\,cm^{-1}}\sigma(\upsilon,P_{air},T) = 1.103\times10^{-18}\,cm\ molecule^{-1}(\pm0.7\%) \quad (2)$$

The value for the integral in Eq. (2) was determined by integrating the three composite PNNL spectra (276, 298 and 323 K) over the wavenumber range 3260–2700 cm^{-1}, taking the average and converting to HITRAN units using the factor $k_B\times296\times\ln\ 10\times10^4/0.101325$. The uncertainty in parentheses represents the spread from the mean of the three PNNL integrated band intensities.

Figs. 1 and 2 display some of the acetonitrile infrared absorption cross sections detailed in Table 2. In Fig. 1 the 3 μm spectral region is shown for the acetonitrile cross section recorded at 207.6 K, with a total pressure of 50.5 Torr. The strongest features are Q branches from the ν_5 band. Future retrievals will require the inclusion of these features in the microwindows. In Fig. 2 a small part (a Q branch centred at $\sim$2985.4 cm^{-1}) of the three absorption cross sections recorded at 217 K are shown depicting the effects of pressure broadening with total pressures of 50.0, 99.4 and 248.5 Torr. It can be observed that the addition of synthetic air leads to significant broadening and a reduction in the sharpness of the lines. Additionally, the acetonitrile absorption features

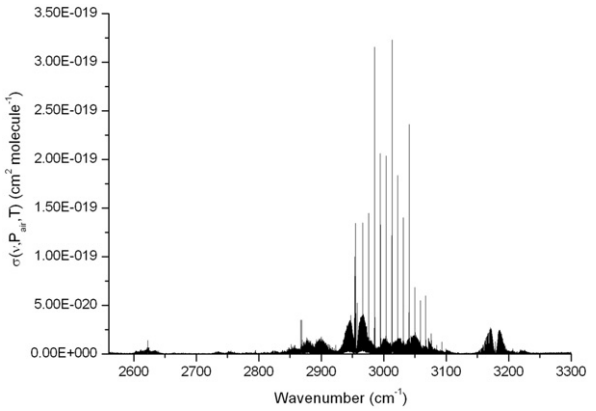

Fig. 1. Air-broadened acetonitrile absorption cross sections showing the spectral range recorded at 207.6 K, with a total pressure of 50.5 Torr. The strong absorption features can be attributed to the *Q* branches of the ν_5 band.

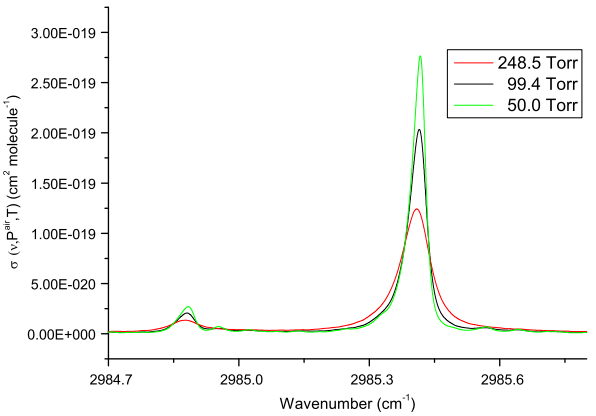

Fig. 2. Three acetonitrile infrared absorption cross sections recorded at 217 K with total pressures of 50.0, 99.4 and 248.5 Torr after the addition of synthetic air (see Table 2 for experimental conditions).

generally become slightly narrower and sharper with decreasing temperature. The spectral absorption cross sections summarised in Table 2 are available electronically upon request from the authors.

4. Conclusions

Eleven air-broadened high resolution acetonitrile spectra, covering the 3 μm region, have been recorded at five different temperatures and various pressures that are representative of conditions in the Earth's atmosphere. The spectra were recorded using the multipass SPAC at RAL. These spectra were used to determine new infrared absorption cross sections, which were calibrated against PNNL integrated band intensities. The cross sections will enable retrievals of acetonitrile from atmospheric spectra recorded by remote sensing instruments on board satellites, such as the ACE-FTS.

Acknowledgements

The authors would like to thank the Natural Environment Research Council (NERC) for supporting N.D.C. Allen through the National Centre for Earth Observation (NCEO), J.J. Harrison through the research grant NE/F002041/1 and for access to the instrumentation at the MSF. We would like to thank R.G. Williams and R. McPheat for their help and assistance throughout the duration of the experimental work carried out at RAL.

References

[1] Hamm S, Warneck P. The interhemispheric distribution and the budget of acetonitrile in the troposphere. J Geophys Res—Atmos 1990;95:20593–606.
[2] Sprung D, Jost C, Reiner T, Hansel A, Wisthaler A. Acetone and acetonitrile in the tropical Indian Ocean boundary layer and free troposphere: aircraft-based intercomparison of AP-CIMS and PTR-MS measurements. J Geophys Res—Atmos 2001;106:28511–27.
[3] Holzinger R, Warneke C, Hansel A, Jordan A, Lindinger W, Scharffe DH, et al. Biomass burning as a source of formaldehyde, acetaldehyde, methanol, acetone, acetonitrile, and hydrogen cyanide. Geophys Res Lett 1999;26:1161–4.
[4] Lobert JM, Scharffe DH, Hao WM, Crutzen PJ. Importance of biomass burning in the atmospheric budgets of nitrogen-containing gases. Nature 1990;346:552–4.
[5] Kuhlbusch TA, Lobert JM, Crutzen PJ, Warneck P. Molecular nitrogen emissions from denitrification during biomass burning. Nature 1991;351:135–7.
[6] Li QB, Jacob DJ, Yantosca RM, Heald CL, Singh HB, Koike M, et al. A global three-dimensional model analysis of the atmospheric

budgets of HCN and CH_3CN: constraints from aircraft and ground measurements. J Geophys Res—Atmos 2003;108:16.
[7] Becker KH, Ionescu A. Acertonitrile in the lower troposphere. Geophys Res Lett 1982;9:1349–51.
[8] Schneider J, Burger V, Arnold F. Methyl cyanide and hydrogen cyanide measurements in the lower stratosphere: implications for methyl cyanide sources and sinks. J Geophys Res—Atmos 1997;102:25501–6.
[9] Singh HB, Salas L, Herlth D, Kolyer R, Czech E, Viezee W, et al. In situ measurements of HCN and CH_3CN over the Pacific Ocean: sources, sinks, and budgets. J Geophys Res—Atmos 2003;108:14.
[10] Arijs E, Brasseur G. Acetonitrile in the stratosphere and implications for positive-ion composition. J Geophys Res—Atmos 1986;91:4003–16.
[11] Kleinbohl A, Toon GC, Sen B, Blavier JFL, Weisenstein DK, Strekowski RS, et al. On the stratospheric chemistry of hydrogen cyanide. Geophys Res Lett 2006;33:5.
[12] Livesey NJ, Waters JW, Khosravi R, Brasseur GP, Tyndall GS, Read WG. Stratospheric CH_3CN from the UARS microwave limb sounder. Geophys Res Lett 2001;28:779–82.
[13] Tyndall GS, Orlando JJ, Wallington TJ, Hurley MD. Products of the chlorine-atom- and hydroxyl-radical-initiated oxidation of CH_3CN. J Phys Chem A 2001;105:5380–4.
[14] de Gouw JA, Warneke C, Parrish DD, Holloway JS, Trainer M, Fehsenfeld FC. Emission sources and ocean uptake of acetonitrile (CH_3CN) in the atmosphere. J Geophys Res—Atmos 2003;108:8.
[15] Jost C, Trentmann J, Sprung D, Andreae MO, Dewey K. Deposition of acetonitrile to the Atlantic Ocean off Namibia and Angola and its implications for the atmospheric budget of acetonitrile. Geophys Res Lett 2003;30:4.
[16] de Laat ATJ, de Gouw JA, Lelieveld J, Hansel A. Model analysis of trace gas measurements and pollution impact during INDOEX. J Geophys Res—Atmos 2001;106:28469–80.
[17] Bange HW, Williams J. New Directions: acetonitrile in atmospheric and biogeochemical cycles. Atmos Environ 2000;34:4959–60.
[18] Livesey NJ, Fromm MD, Waters JW, Manney GL, Santee ML, Read WG. Enhancements in lower stratospheric CH_3CN observed by the upper atmosphere research satellite microwave limb sounder following boreal forest fires. J Geophys Res—Atmos 2004;109:9.
[19] Arijs E, Ingels J, Nevejans D. Mass-spectrometric measurement of positive-ion composition in the stratosphere. Nature 1978;271:642–4.
[20] Arijs E, Nevejans D, Ingels J. Positive-ion composition measurements and acetonitrile in the upper-stratosphere. Nature 1983;303:314–6.
[21] Arnold F. Multi-ion complexes in the stratosphere—implications for trace gases and aerosol. Nature 1980;284:610–1.
[22] Sanhueza E, Holzinger R, Kleiss B, Donoso L, Crutzen PJ. New insights in the global cycle of acetonitrile: release from the ocean and dry deposition in the tropical savanna of Venezuela. Atmos Chem Phys 2004;4:275–80.
[23] Watson C, Churchwell E, Pankonin V, Bieging JH. Arcsecond images of CH_3CN toward W75N. Astrophys J 2002;577:260–4.
[24] Zhang QZ, Ho PTP, Ohashi N. Dynamical collapse in W51 massive cores: CS (3-2) and CH_3CN observations. Astrophys J 1998;494:636–56.
[25] Marten A, Hidayat T, Biraud Y, Moreno R. New millimeter heterodyne observations of Titan: vertical distributions of nitriles HCN, HC_3N, CH_3CN, and the isotopic ratio N-15/N-14 in its atmosphere. Icarus 2002;158:532–44.
[26] Nishio M, Paillous P, Khlifi M, Bruston P, Raulin F. Infrared-spectra of gaseous ethanenitrile in the 3500–250 cm^{-1} region—absolute band intensity and implications for the atmosphere of Titan. Spectrochim Acta A—Mol Biomol Spect 1995;51:617–22.
[27] Anttila R, Horneman VM, Koivusaari M, Paso R. Ground-state constants A_0, D_0^K and H_0^K of CH_3CN. J Mol Spectrosc 1993;157:198–207.
[28] Huet TR. The v_1 and v_5 fundamental bands of methyl cyanide. J Mol Struct 2000;517:127–31.
[29] Tolonen AM, Koivusaari M, Paso R, Schroderus J, Alanko S, Anttila R. The infrared spectrum of methyl cyanide between 850 and 1150 cm^{-1}: analysis of the v_4 band, v_7 band, and $3v_8^1$ bands with resonances. J Mol Spectrosc 1993;160:554–65.
[30] Rinsland CP, Sharpe SW, Sams RL. Temperature-dependent infrared absorption cross sections of methyl cyanide (acetonitrile). J Quant Spectrosc Radiat Transf 2005;96:271–80.
[31] Rinsland CP, Devi VM, Benner DC, Blake TA, Sams RL, Brown LR, et al. Multispectrum analysis of the v_4 band of CH_3CN: positions, intensities, self- and N_2-broadening, and pressure-induced shifts. J Quant Spectrosc Radiat Transf 2008;109:974–94.
[32] Rothman LS, Gordon IE, Barbe A, Benner DC, Bernath PF, Birk M, et al. The HITRAN 2008 molecular spectroscopic database. J Quant Spectrosc Radiat Transf 2009;110:533–72.
[33] Bernath PF, McElroy CT, Abrams MC, Boone CD, Butler M, Camy-Peyret C, et al. Atmospheric Chemistry Experiment (ACE): Mission overview. Geophys Res Lett 2005;32:5.
[34] Paynter DJ, Ptashnik IV, Shine KP, Smith KM, McPheat R, Williams RG. Laboratory measurements of the water vapor continuum in the 1200–8000 cm^{-1} region between 293 K and 351 K. J Geophys Res—Atmos 2009;114:23.
[35] Harrison JJ, Allen NDC, Bernath PF. Infrared absorption cross sections for acetone (propanone) in the 3 μm region. J Quant Spectrosc Radiat Transf 2011;112:53–8.